

Design of a high torque, lightweight clutch for use in an exoskeleton to augment human running

by

Andrew T. Marecki

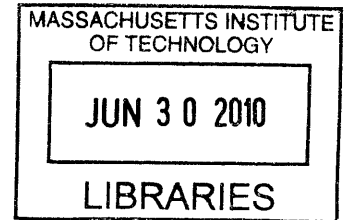
SUBMITTED TO THE DEPARTMENT OF MECHANICAL ENGINEERING IN PARTIAL FULLFILLMENT OF THE REQUIREMENTS FOR THE DEGREE OF

BACHELOR OF SCIENCE IN MECHANICAL ENGINEERING AT THE MASSACHUSETTS INSTITUTE OF TECHNOLOGY

JUNE 2010

© 2010 Andrew T. Marecki. All rights reserved.

The author hereby grants to MIT permission to reproduce and to distribute publicly paper and electronic copies of this thesis document in whole or in part in any medium now known or hereafter created.



ARCHIVES

Signature of Author: _____ Department of Mechanical Engineering May 10, 2010

Certified by: _____ Hugh M. Herr Professor of Media Arts and Sciences Thesis Supervisor

Accepted by: _____ John H. Lienhard V Senior Professor of Mechanical Engineering Chairman, Undergraduate Thesis Committee

Design of a high torque, lightweight clutch for use in an exoskeleton to augment human running

by

Andrew T. Marecki

Submitted to the Department of Mechanical Engineering
on May 10, 2010 in Partial Fulfillment of the
Requirements for the Degree of Bachelor of Science in
Mechanical Engineering

ABSTRACT

The metabolic augmentation of human locomotion through the use of wearable exoskeletons is a complex and difficult goal. One exoskeleton architecture adds parallel elasticity to the user during stance phase to unload the user's muscles and joints. Critical to this design is the creation of a lightweight, high torque clutch that can endure the forces associated with ground impact and stance phase in running and also disengage to permit a natural swing phase. The clutch makes use of radial, ratcheting clutch plates, a planetary gearbox, and a novel mechanical decoupling concept to meet the design requirements.

Thesis Supervisor: Hugh M. Herr
Title: Professor of Media Arts and Sciences

1. Introduction

An exoskeleton that augments human running would revolutionize how we think of the human body. Perfecting the grace and efficiency of the human form is one of the primary purposes of these technologies. No passive or quasipassive wearable exoskeleton has yet demonstrated a reduction in metabolic demand. One exoskeleton concept uses leaf springs in parallel with the legs and a clutched knee joint. This paper explains the design of the lightweight, low power, high torque clutch used for this exoskeleton architecture.

1.1 Basic Biomechanics of Running

Running gaits are characterized by the use of spring-like limbs which store and return kinetic and gravitational potential energy to the body. Early stance phase begins with foot strike, which is followed by knee flexion and ankle dorsiflexion of the respective limb. Ground reaction force increases until midstance, when the body's center of mass is above the foot, typically reaching as much as three body weights at speeds of 3 to 5 m/s [1]. After midstance, the limb is gradually unloaded until toe off. Swing phase occurs after toe off and involves hip flexion, which brings the leg forward. The knee is simultaneously flexed to reduce the leg's moment of inertia about the hip. The knee is extended just before foot strike during terminal swing.

The proposed exoskeleton is designed to provide parallel stiffness at strike and throughout stance phase. This would decrease the observed loads of the muscles that hold the quadriceps and Achilles tendons in place. These reductions in required isometric muscle force could yield a decline in overall metabolic energy consumption. The knee clutch needs to sustain the dynamic radial and torsional loads associated with running in its locked state, as well as allow an uninhibited swing phase in its unlocked state.

1.2 Clutch Specifications

The design specifications of this clutch include strict requirements on torque, resolution, and weight. The human knee experiences torques of up to 200 Nm at midstance, so the clutch must support this load at minimum. This estimate is conservative in itself, as both the exoskeleton and the human musculoskeletal system will bear the forces associated with running.

Slip within the device is not tolerated, as any such movements will decrease the overall elastic energy storage of the exoskeleton. The clutch must have a resolution of less than five degrees. The device should ideally lock at maximum knee extension before foot strike, and locking at lesser angles represents a loss of potential energy storage and return.

1.3 Clutching Options

A number of clutching options were investigated, including particle brakes, friction plates, hydraulic brakes, and toothed surfaces. Figure 1 displays over 350 commercially available clutches, organized by their mass and maximum holding torque. No clutches capable of supporting 200 Nm exist at masses less than 1 kg. The large dot on the plot is the design configuration that was achieved in this study.

Friction brakes were not a viable option because the impulses at ground impact would cause the clutch plates to slip. While friction brakes could potentially resist the high impacts at toe strike, the normal force required to achieve this performance is unreasonably high and cannot be generated in a lightweight, compact manner. Cam based variants had issues similar to those of friction clutches.

Hydraulic brakes did not satisfy the design criteria either. While hydraulic systems certainly could provide the desired holding forces, they are prohibitively heavy. The bulk of this mass comes from the essential compressor, which would likely be placed at the hip to minimize distal mass of the exoskeleton.

Ratchets were eliminated because only one tooth experiences the entire applied force. Under the extremely high stresses at ground impact, the ratchet teeth would zipper off. All of the options to increase the ratchet's holding torque would make it less optimal for the target application. Increasing tooth size would decrease the clutch's resolution and using multiple pawls would increase complexity and mass. A system using multiple pawls requires all of the mechanisms to be simultaneously disengaged before movement in the opposite direction is allowed. Increasing the ratchet's diameter would linearly decrease the resulting tooth forces, but at the cost of quadratically increasing mass.

Other toothed clutch plates were also investigated in detail. This design involves the use of meshing plates in which all of the features engage simultaneously. Thus, large shear area of resistance is achieved, which can effectively handle the specified torque. Furthermore, the

desired resolution can be realized if the radial teeth are fine enough. A toothed design was chosen as the best torque resisting option. In particular, a dog clutch design with angled teeth was implemented.

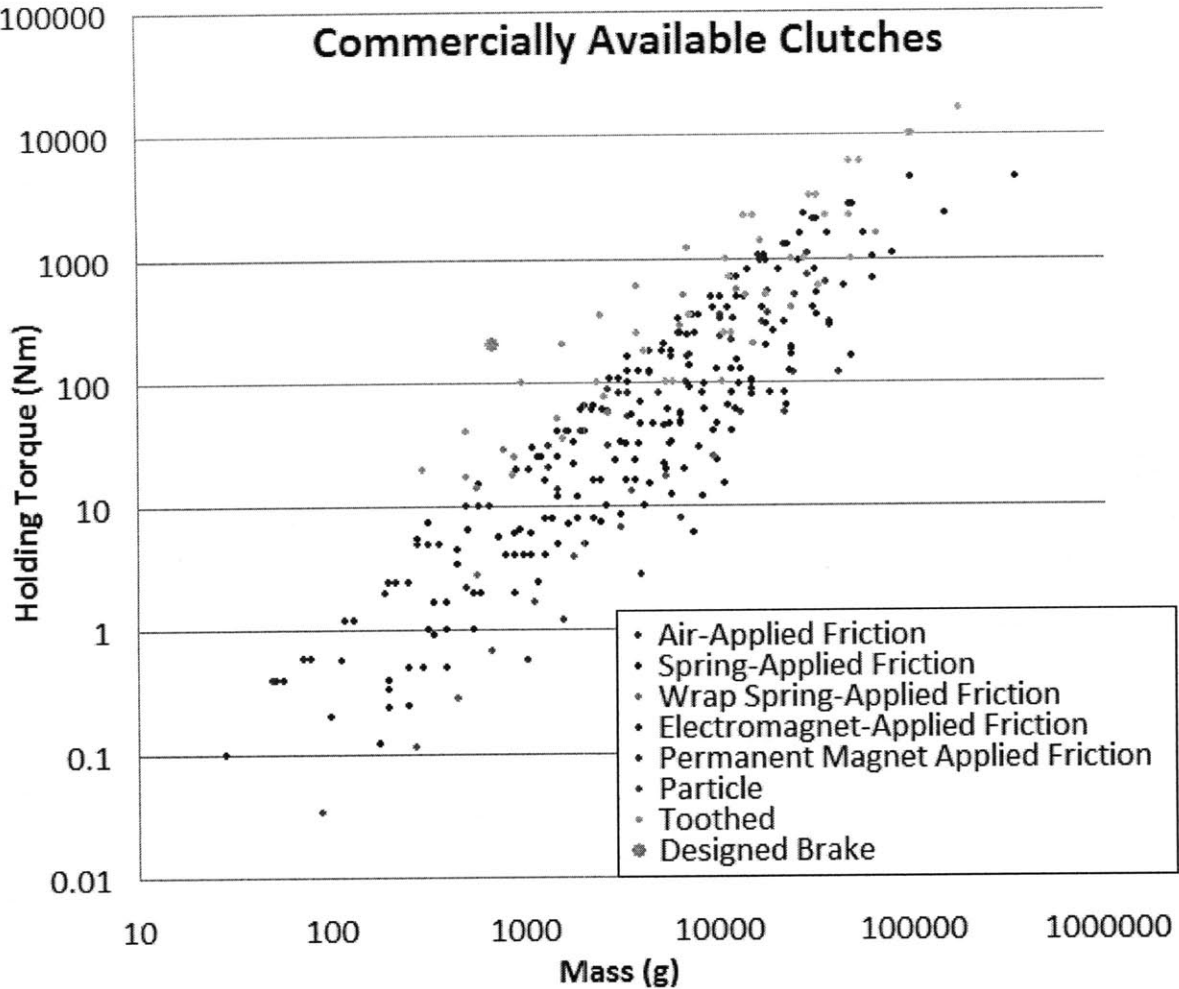
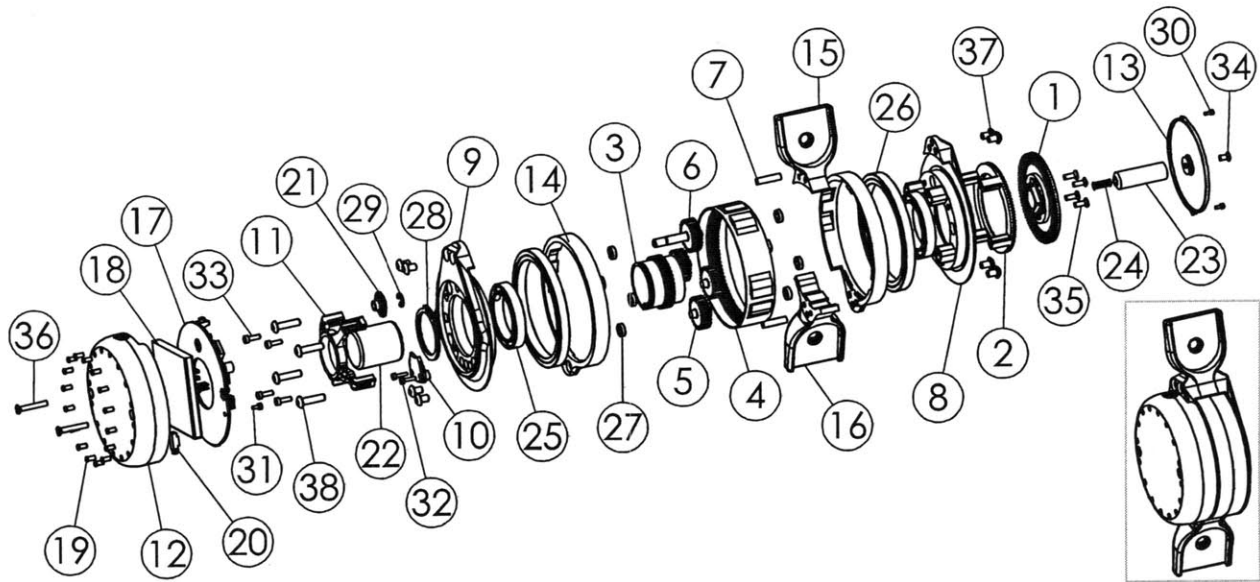


Figure 1: Log-log plot of commercially available clutches. Notice how the designed clutch is half the mass of its best competitor at the required holding torque and has twice the holding torque of the best device at a similar mass.

2. Device Design

The designed device uses angled radial dog teeth on the clutch plates for torque resistance and a planetary gear system to more than double the device's clutching resolution. Figure 2 presents an exploded view of the clutch and figure 3 displays several breakdown views of the assembled device.



Item No.	Name	Material	Mass (g)	Quantity
1	Rotating Clutch Plate	Titanium Grade 2	28.6	1
2	Translating Clutch Plate	Titanium Grade 5	18.7	1
3	Sun Gear	Titanium Grade 5	22.5	1
4	Ring Gear	Titanium Grade 5	48.9	1
5	Planet Gear	Titanium Grade 2	8.3	3
6	Long Planet Gear	Titanium Grade 2	9.9	1
7	Pin	Titanium Grade 2	0.9	2
8	Medial Planet Carrier	Aluminum 6061	49.5	1
9	Lateral Planet Carrier	Aluminum 6061	57.8	1
10	Hard Stop	Aluminum 6061	2.2	1
11	Solenoid Mount	Aluminum 6061	8.6	1
12	Lateral Cap	Aluminum 6061	38.1	1
13	Medial Cap	Aluminum 6061	6.5	1
14	Distal Ear	Aluminum 6061	20.3	2
15	Proximal Mount	Aluminum 6061	32.6	1
16	Distal Mount	Aluminum 6061	36.6	1
17	Circuit Board	(Multiple)	25	1
18	Lithium Polymer Battery	(Multiple)	16.8	1
19	Light Pipe	Acrylic	0.0	16
20	Right Angle Light Pipe	Acrylic	0.2	1
21	EP4 Optical Encoder Disk	Aluminum 6061	3.0	1
22	LT8x9 Solenoid	Brass and Copper	55.0	1
23	Solenoid Plunger	Ductile Iron	22.6	1
24	Solenoid Return Spring	Steel	0.2	1
25	Sun Bearing	Steel AISI304	20.0	2
26	Ring Bearing	Steel AISI304	56.8	2
27	Planet Bearing	Steel 440C	0.5	8
28	Retaining Ring	Cast Carbon Steel	3.7	1
29	E-Clip	Cast Carbon Steel	0.2	1
30	M1.6x0.35x4 Cap Screw	Steel	0.5	2
31	M2x0.4x4 Cap Screw	Steel	0.3	2
32	M2x0.4x8 Cap Screw	Steel	0.4	2
33	M2.5x0.45x8 Cap Screw	Steel	0.7	4
34	M3x0.5x6 Flat Head Screw	Steel	0.5	1
35	M3x0.5x8 Flat Head Screw	Steel	0.6	4
36	M3x0.5x22 Flat Head Cap Screw	Steel	1.4	2
37	M4x0.7x6 Cap Screw	Steel	1.2	8
38	M4x0.7x16 Cap Screw	Steel	2.3	4

Figure 2: Exploded view of the clutch with assembled view shown and bill of materials.

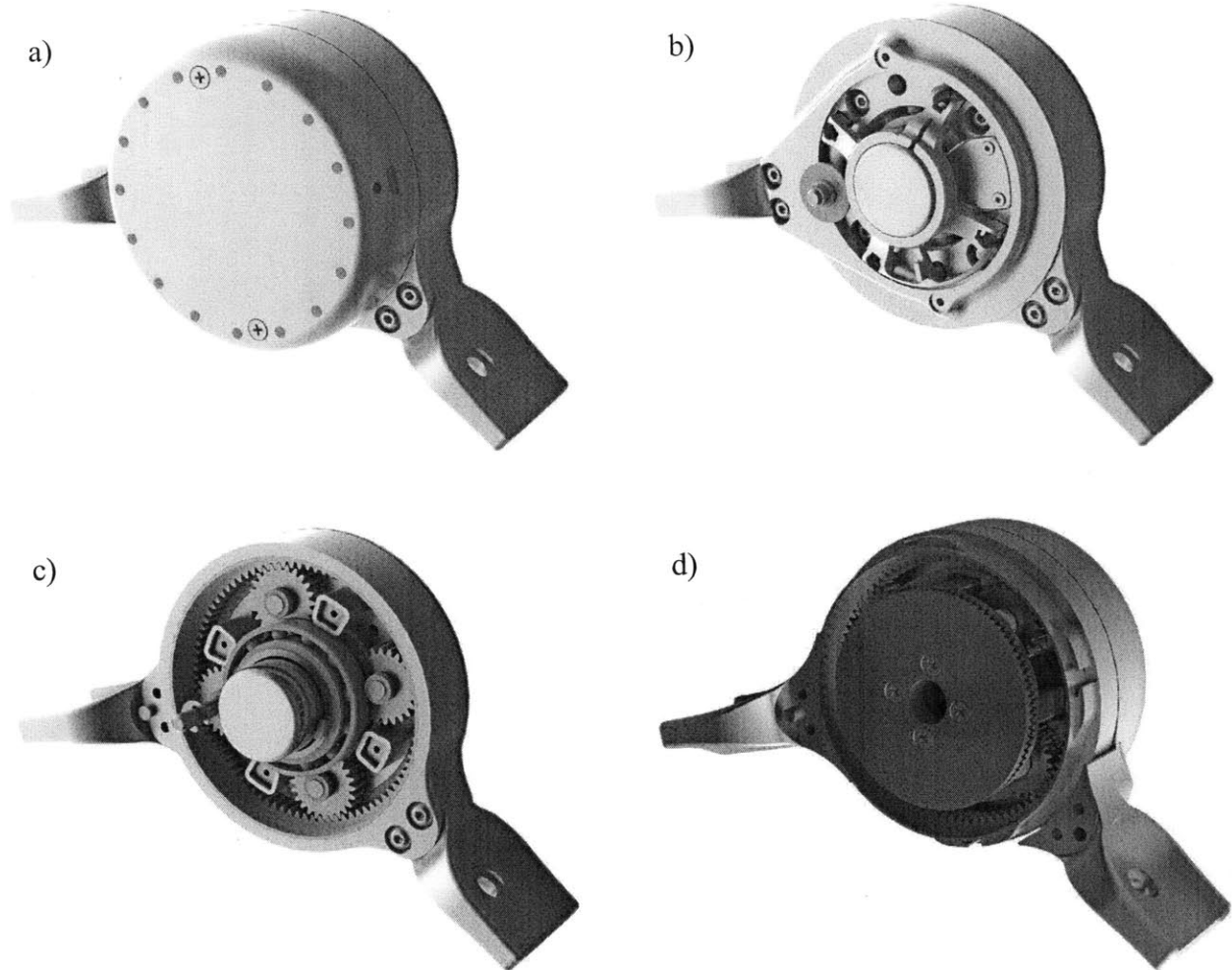


Figure 3: Rendered views of the right side clutch. a) Complete clutch. b) Removal of the lateral assembly reveals the solenoid, solenoid mount, and reflective encoder. c) Removal of the lateral planet carrier displays the planetary system. d) Medial parts removed from opposite side shows the disengaged clutch plates.

The planetary gearbox is critical to realizing several important design specifications. The resolution of the clutch plates is limited to around 4° , due to ball mill size restrictions in contour milling. Also, the clutch must be able to disengage at non-zero torques. The planetary multiplies the effective resolution of the system by increasing the angular velocity of the rotating clutch plate. The small amount of backlash in the gear system provides enough play for the clutch plates to disengage at non-zero torques.

Another important part of the mechanical design is the combination of linear and rotary motions that provide clutching. In this device, the proximal subassembly, including the planet carrier, is assumed to be fixed, and the rotation of the distal mount is coupled to the rotation of one of the clutch plates via the planetary system. The other clutch plate is linearly actuated within the rigid planet carrier between clutched and unlocked states. In the clutched state, the linearly translating clutch plate is meshed with the rotating clutch plate, so the sun, ring, and planet carrier are all fixed with respect to one another. The unlocked state offers no constraints on the device, so all of the elements of the planetary drive are free to rotate. Figure 4 shows the clutch plates; one passes through the planetary drive, while the other is attached to the sun gear.

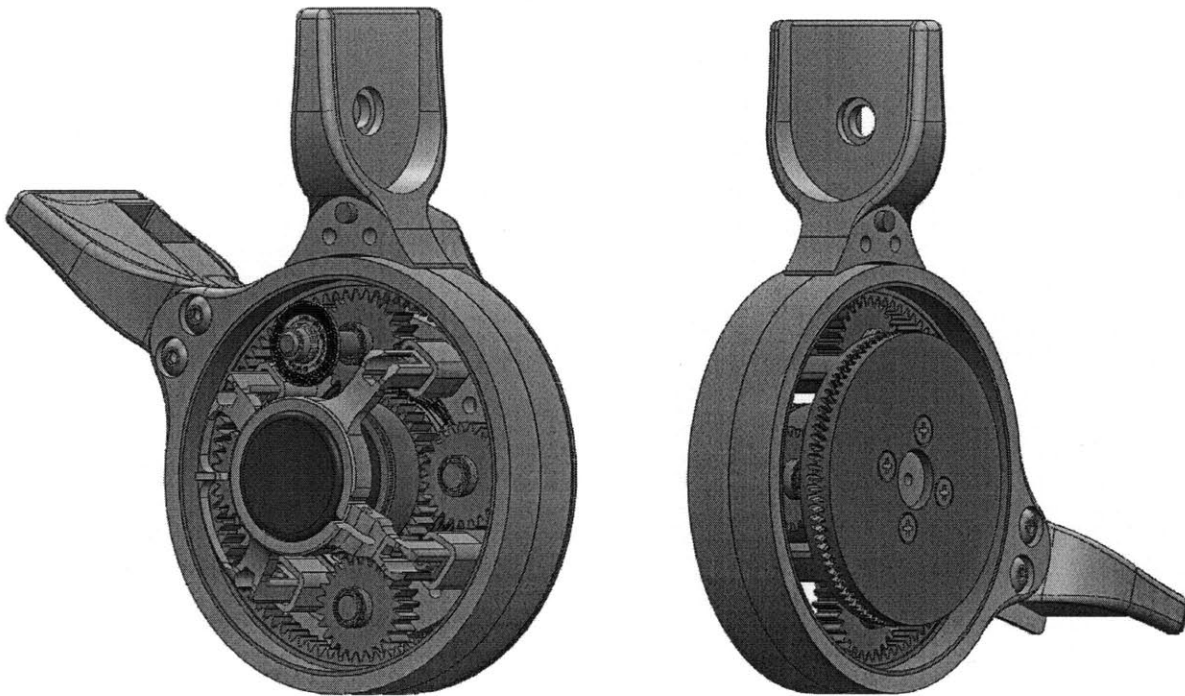


Figure 4: Views showing the clutch's internal mechanisms. The left view shows the planetary system and half of the planet carrier, while the right shows the clutch plates. The left plate is fixed to the solenoid mount and only translates. The right plate is fixed to the sun and only rotates.

2.1 Clutch Plates

The core of the mechanical design lies in the two clutch plates, which serve to lock the knee joint at peak extension shortly before toe strike and for the duration of stance phase. Only at terminal stance are the clutch plates disengaged, when the solenoid is shut off and the return spring overcomes the binding friction at the interface.

A dog clutch couples two rotating surfaces via mechanical interference, rather than by the use of friction. The use of radial teeth that all engage with the mating clutch plate offers an entire shear area of resistance. This means that the clutch plates will never slip or fail unless all of the teeth are plastically deformed simultaneously. If the plates are engaged at low speeds, there will be minimal wear in the system. No wearing effects occur when the teeth are completely meshed and under load.

An angled tooth profile was chosen to offer the possibility of ratcheting between the two mating plates. The ratcheting option means that the clutch can be engaged during terminal swing phase and still offer knee movement in the extension direction. This is not the ideal control strategy as it incurs losses, but it ensures that the device will always be able to perform the desired action. The desired usage model requires that the clutch locks at maximum knee angle just before toe strike in running. If locking occurs anytime after toe strike, all of the potential energy storage is lost and metabolics are impacted significantly by the fact that the user is carrying the mass of the exoskeleton and not gaining any benefits. While a castle tooth configuration could offer similar torque resistance, it lacks the ratcheting option. Figure 5 details the lofted tooth profile of one of the clutch plates.

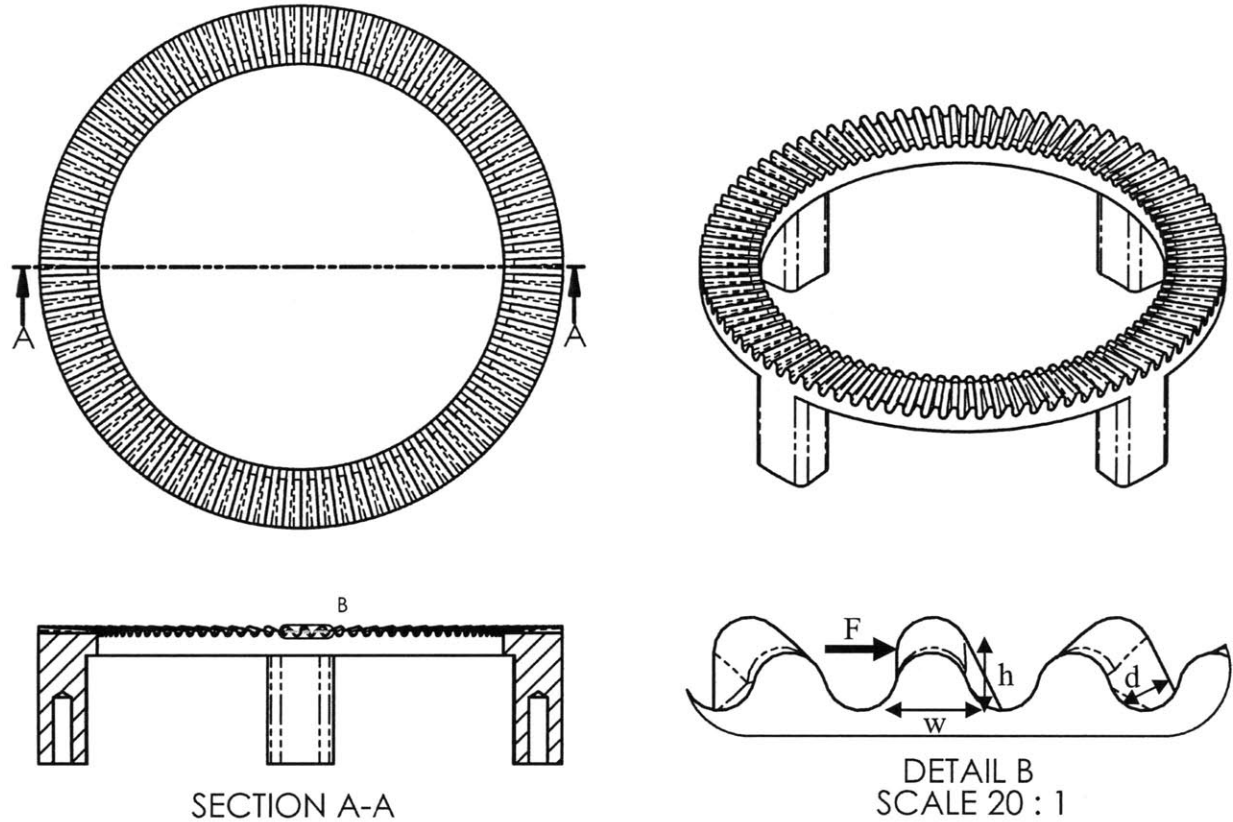


Figure 5: Drawing of the translating clutch plate with Section A-A and Detail B showing the tooth profile.

Basic bending and shear equations were used to determine the strength of the clutch teeth. With this design, the required torque resistance is approximately 90 Nm because a 2.2:1 planetary gearbox is used in the system. The planetary serves to decrease the torque seen by the clutch plates, which allows to smaller teeth at finer resolutions. With an ultimate tensile strength comparable to many steels and a density that is about 45% less than steel, titanium is the ideal material for these components. Two different titanium alloys, grade 2 and 5, were used for the clutch plates to maximize their strength to weight ratio and avoid galling effects.

Under optimal conditions where the clutch plates are fully engaged, the maximum applied torque can be determined if the plates fail in shear by equation 1 [3].

$$\tau_{\max} = \pi(r_{\text{outer}}^2 - r_{\text{inner}}^2) \sigma_{\text{UTS}} r_{\text{inner}} = \pi((0.029\text{m})^2 - (0.0225\text{m})^2) (490\text{MPa})(0.0225\text{m}) = 11.6\text{kNm} \quad (1)$$

The yield stress of grade 2 titanium is 490 MPa and grade 5 is 830MPa [4]. The above calculation shows the fully engaged clutch plates will never fail in shear. It is independent of tooth size, as it only relies on the total shear area.

Tooth bending is the more likely failure condition for the clutch plates. The tip fillet on each tooth prevents partial engagement at the very end as forces at this interface would produce a thrust force that pushes the plates apart. It is conceivable, however, that the clutch plates may be loaded when the teeth are only half meshed. Root fillets are also used to relieve stress concentrations at the base of each tooth. A lofted tooth profile, visible in figure 5, is implemented in this design due to the radial orientation of the teeth. In the radially outward direction, the profile becomes larger and deeper as the sector for each tooth widens. This profile makes it such that more of the applied forces are resisted at larger diameters, than at smaller ones, so no one region yields before the others. Each clutch plate contains 90 teeth that are approximately 2 mm wide, 1.5 mm tall, and 6.5mm deep. For the purposes of a simple bending calculation, the area moment of inertia of a single tooth can be approximated by equation 2, which is the area moment of inertia of a rectangular cross section.

$$I_{tooth} = \frac{dw^3}{12} = \frac{(0.0065m)(0.002m)^3}{12} = 4.33 \times 10^{-12} m^4 \quad (2)$$

The maximum torque that can be applied to the clutch at half engagement can be approximated by equation 3, which depends on the material properties and tooth geometry [3].

$$\tau_{max} = \frac{n_{gear_ratio} n_{teeth} I_{tooth} \sigma_{UTS}}{h/2} = \frac{(2.2)(90)(4.33 \times 10^{-12} m^4)(490MPa)}{0.00075m} = 560Nm \quad (3)$$

Even under worst case conditions, the clutch plates will not fail. The clutch's overall holding torque is over twice the design requirement. Furthermore, it is unlikely that the plates will experience high loads under partial engagement as the tip fillets will cause a thrust force that pushes the plates apart if they are not fully meshed.

The clutch plates are contour milled with tolerances of +/- 5×10^{-4} inches (+/- 1.3×10^{-5} m). This tolerance means that all of the teeth will engage before any one fails. Equation 4 details the calculation of the maximum tooth deflection if the entire load is placed on one tooth under partial engagement. This deflection is almost exactly the same as the machining tolerance.

$$\delta_{bending} = \frac{Fh^3}{3E_{Ti} I_{tooth}} = \frac{(100Nm / 0.0225m)(0.0015m)^3}{3(105GPa)(4.33 \times 10^{-12} m^4)} = 1.1 \times 10^{-5} m \quad (4)$$

Therefore, all of the teeth will elastically deform before any single tooth yields. This estimate of maximum deflection before yield is also an underestimate, because an upper bound on the area moment of inertia of a single tooth is used here. In reality, the deflection will be

greater because the inertia decreases at successively higher cross sections. This also means that the bending stress will be slightly higher than predicted in equation 3, but the teeth will not yield. Figure 6 shows the designed tooth profile and the mesh between the two clutch plates. The tooth size is determined by the availability of tooling. The root fillets have 1/64 inch radii, which can be contour milled using a 1/32 inch diameter ball mill.

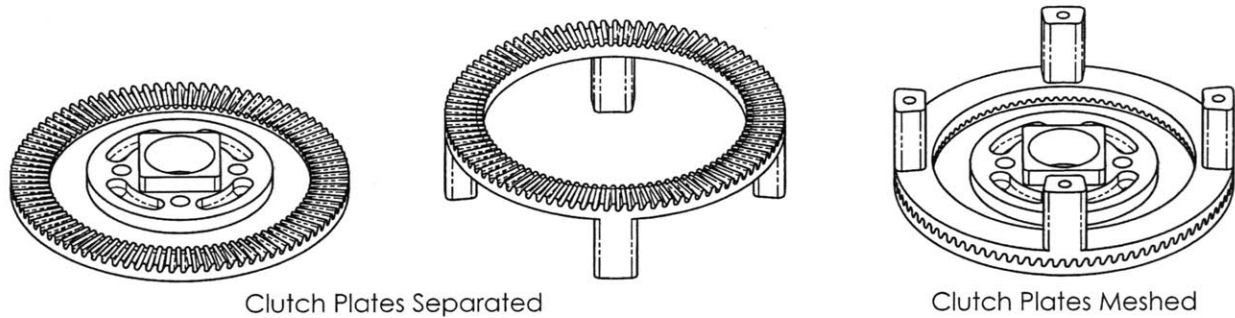


Figure 6: Separate and meshed views of the two clutch plates.

Wear between the clutch plates is limited by the use of lubricants and the usage pattern of the clutch. As aforementioned, the clutch plates are meshed at low angular velocities, ideally when the joint's angle reaches its maximum value and the angular velocity is zero. Therefore, no synchronizer mechanism is required to prevent the clutch plates from excessive grinding as they mesh. The machined titanium plates were lightly bead blasted after machining to remove any imperfections in the surfaces. Also, both plates were coated by a thin film of dry PTFE lubricant which limits wear, improves ratcheting, and has no suction effects. This type of lubricant is also non-conductive, which is an important consideration for a dense electromechanical system. A wet lubricant would cause the precision machined clutch plates to stick together once meshed, making it difficult to disengage the mechanism.

2.2 Planetary Gearbox

The clutch also makes use of a planetary gearbox to increase the clutch's effective resolution and decrease the torque observed by the clutch plates. A 2.2:1 transmission ratio between the sun and ring gear is implemented here, where the sun is fixed to the rotating clutch plate, the planet carrier is attached to the proximal link of the exoskeleton, and the ring is attached to the distal mount. Thus, the distal subassembly, linked to the lower leg, rotates

relative to the proximal subassembly, which is fixed to the upper leg. In this configuration, the planet carrier is fixed, the ring is the input, and the sun is the output. Figure 7 illustrates the planetary gearbox and the involute tooth profile. A 2.2:1 gear ratio is achieved with this four planet configuration. This ratio not only provides the benefits noted above, but also meets the design constraints of accommodating the 25.6 mm diameter solenoid concentric with the sun as well as the proper bearings at the ring's inner surface. The sun, planets, and ring have 40, 24, and 88 teeth, respectively, all at a metric tooth module of 0.8. These tooth numbers are all divisible by four, which permits the symmetric meshing of four planets. Four planets were necessary to distribute the applied torque, and a module of 0.8 provided a balance between the number of meshing teeth at any given time and tooth size.

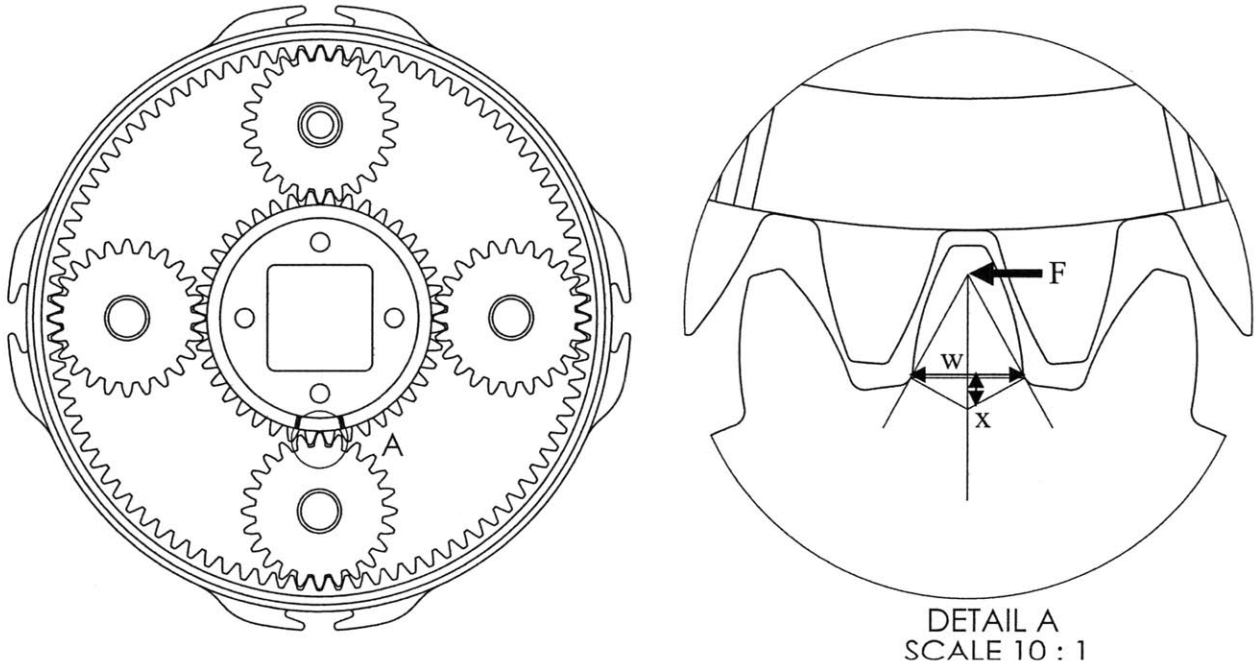


Figure 7: Drawing of the planetary system and detail view of the tangential force on one tooth.

Bending and shear calculations, similar to equations 1, 2, and 3 were employed to calculate the maximum gear tooth load. Equation 5 calculates the torque at failure for shear, where w is the tooth width,

$$\tau_{\max} = \sigma_{UTS} w d r_{ring} n_{engaged} = (490MPa)(0.0015m)(0.006m)(0.0704m)(8) = 2484Nm \quad (5)$$

The likely failure mode for the gear teeth is in bending, rather than shear. Equation 6 presents the Lewis bending equation for gear tooth failure, and equation 7 solves this formula for the maximum supported torque of the clutch [2]. Here F is the tangential force applied to one

tooth, which is equal to the applied torque divided by the moment arm, the ring's radius, and the typical number of engaged teeth. The length x is the vertical distance from the root to the intersection of the lines normal to the root fillets. It depends on the location of the applied force, which is placed at a typical height in figure 7.

$$\sigma = \frac{Fp}{2d xp / 3} = \frac{3\tau}{2dx r_{ring} n_{engaged}} \quad (6)$$

$$\tau_{max} = \frac{2}{3} \sigma_{UTS} r_{ring} n_{engaged} wx = \frac{2}{3} (490MPa)(0.035m)(8)(0.006m)(0.0006m) = 330Nm \quad (7)$$

In actual use, two to three teeth on every planet will be in contact the ring, with the same being true for the sun. Therefore, the planetary will be able to support more than the torque estimate of equation 7.

The planets are composed of grade 2 titanium, while the ring and sun are grade 5. All of the gears were manufactured by precision wire electrical discharge machining (EDM) with a tolerance of 0.0005 inches and lightly bead blasted to remove any imperfections. Figure 8 shows the planetary assembly, complete with bearings and the planet carrier structure.

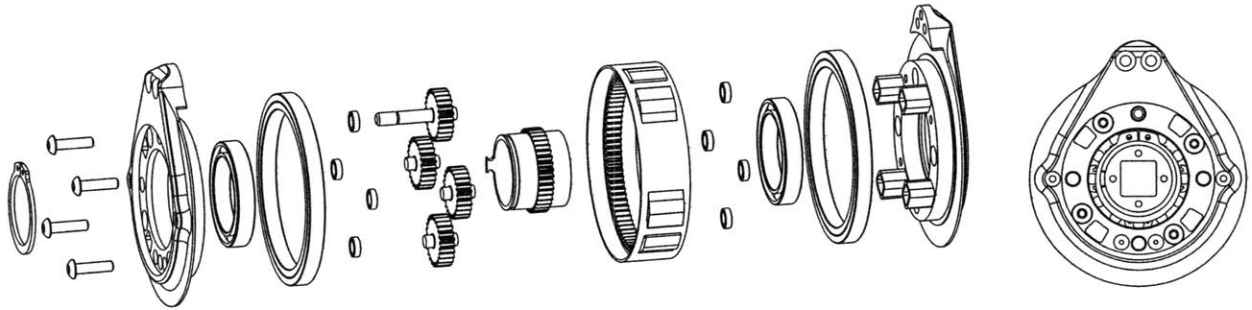


Figure 8: Exploded view of the planetary assembly (left) and assembled front view (right).

2.3 Planetary Carrier and Bearing Selection

The two planet carrier plates hold a total of twelve bearings that maintain the gear positions and reduce rolling resistance under load. The planet carriers are connected by four mating bosses, which add significant structural rigidity in torsional, bending, and shear loading conditions. Four M4 machine screws hold the carriers in compression, while experiencing no other forces. A retaining ring that sits against the inner race of the sun bearing is used to maintain the sun's position within the planetary, including when it experiences thrust forces due to solenoid actuation.

The two ring bearings are subjected to the highest forces of the planetary system, including the radial loads during stance phase which are typically around three times bodyweight. A conservative estimate for the dynamic radial load rating of each bearing is approximately 400 lbs (1800 N). Only multi-load ball bearings were available in the proper form factor to fit within the ring, so the interfaces were designed to use these bearings in a single angular contact configuration, rather than in both angular configurations which could lead to over-constraint. Figure 9 shows section views of the entire clutch. Notice the multiple sets of bearings that support the planetary gearbox as well as the density of this design.

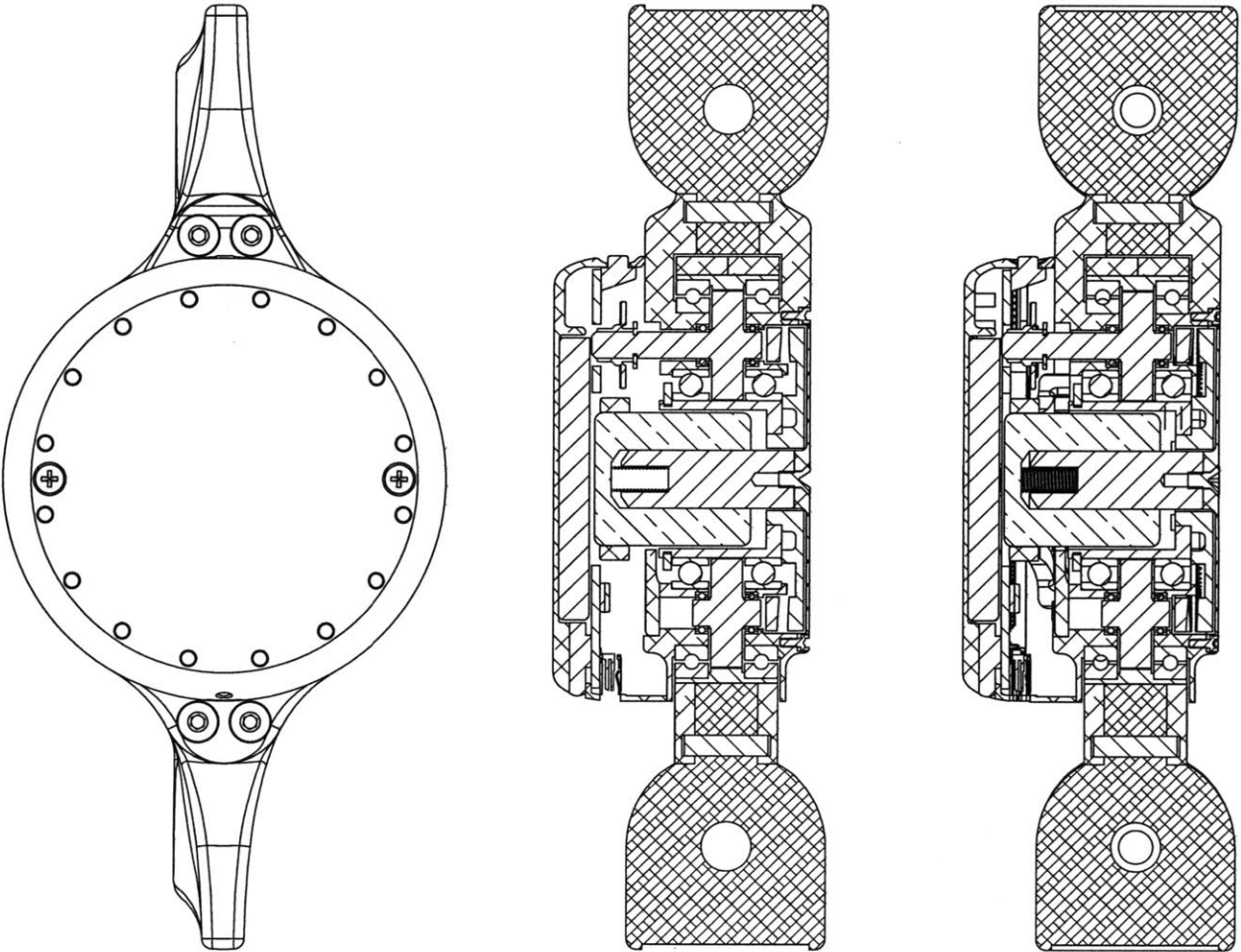


Figure 9: Side view of clutch (left), section view with only cut faces shown (center), and section view with all components shown (right).

The ring bearing is shown to be loaded on its inner race by the planet carrier and on its outer race by a step in the ring gear. This bearing configuration resists both thrust and radial forces, which the clutch will experience in its operation. The outer ring bearings serve to transmit forces across the entire clutch without affecting the planets and sun. The planet bearings only experience radial loads when the clutch is locked and the sun cannot rotate. The sun is rigidly fixed to the rotating clutch plate via a mating square boss and four M3 machine screws. The engagement of the two clutch plates therefore restricts the sun's rotation. When the clutch is loaded in this configuration, the planet carrier exerts a radial load on each of the planets. This maximum dynamic radial load is calculated by equation 8.

$$F_{bearing} = \frac{\tau_{max}}{n_{bearings} r_{planet_orbit}} = \frac{200Nm}{(8)(0.0256m)} = 977N \quad (8)$$

Each of the eight planet bearings must have a dynamic radial load of at least 977 N, which is approximately 220 lbs. The planets are not restricted axially, but instead have steps which touch the inner races of the planet bearings. Furthermore, the planets experience only torsional and radial loads, so thrust resistance is not a problem. The sun is almost completely isolated, as it only undergoes torsional loading. Two radial bearings are used to minimize damping in the system and keep the rotating clutch plate true as it is cyclically meshes and separates from the translating clutch plate.

2.4 Attachment Points

One important aspect of the design is preserving paths for part upgrades and replacement. Although all of the parts were designed to withstand the various loading conditions, unforeseen problems frequently arise in prototype hardware. The clutch is designed in such a way that the only chiral parts are the clutch plates. All of the other parts, including the circuit board can be appropriately positioned to create either a left or right configuration.

Furthermore, the proximal and distal mounts (parts 15 and 16 in figure 2) can be easily swapped out for other mounting options. The exoskeleton currently uses fiberglass leaf springs with rectangular cross sections as its load bearing structure, but these are heavy and slow to interchange. Carbon fiber rods with the same outer diameter but varying inner diameters offers significantly reduced weight at similar stiffnesses, depending on geometry. Modular mounts that clamp these carbon fiber rods can replace the current mounts, increasing this device's versatility.

The mounts can also be switched out for ones that accommodate attachment to knee braces. Rather than being a part of an exoskeleton, the device could serve to clutch a knee brace, reducing the loads on the human knee during stance phase. This can help those with muscle weakness and knee problems.

2.5 Hard Stops

The clutch must operate only in a range similar to the human knee. Figure 10 shows the configurations of the clutch at the extremes of full extension and full flexion, respectively. This range is restricted by the implementation of an achiral hard stop system. At both extremes, a tab on the sun gear contacts a machined aluminum part, which is fixed to the lateral planet carrier. As the distal mount rotates clockwise, the sun rotates counterclockwise at a faster angular rate due to the planetary drive. While the distal mount and therefore the ring gear travel 130° , the sun rotates 286° . A sun tab angle of 24° and a hard stop angle of 48° accommodates this range of travel. The only difference between the left and right clutches is the direction of rotation of the mounts, and therefore the sun. Thus, the sun tab must be put on the appropriate side of the hard stop during assembly, but achirality is maintained.

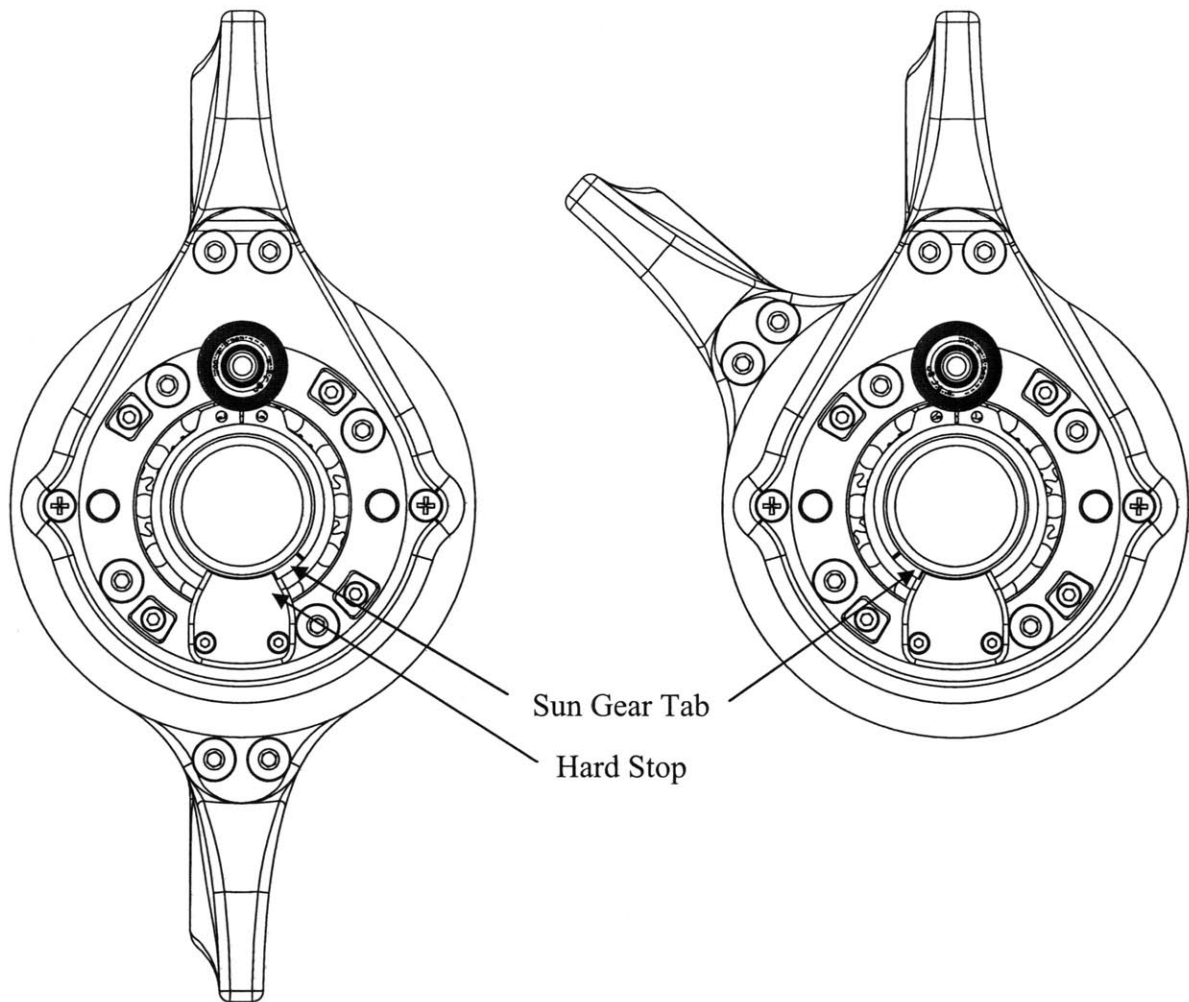


Figure 10: Clutch extended (left) and flexed (right) configurations. Note the tab on the sun gear that contacts the hard stop at both extremes.

Although the hard stop should never be loaded, it is rated for relatively high loads if such a situation arises. Ideally the fiberglass struts of the exoskeleton are selected to avoid knee inversion at maximum knee flexion and ankle plantarflexion. The stop is mainly implemented to prevent knee inversion, and is integrated into the inside of the clutch to avoid any pinch points. The hard stop and corresponding sun gear tab have mating semicircular surfaces, which provide a minimum energy configuration for the mate. Any small disturbances, which should not be present in the system due to the bearing configurations, will have no effect on the hard stop's performance. Both parts are low profile and designed to load in shear, not bending. Equation 9 calculates the maximum torque applied to the clutch that the titanium sun gear tab can sustain.

$$\tau_{\max} = n_{\text{gear_ratio}} A_{\text{tab}} \sigma_{\text{UTS}} r_{\text{sun}} = (2.2)(8 \times 10^{-6} \text{ m}^2)(830 \text{ MPa})(0.01325 \text{ m}) = 194 \text{ Nm} \quad (9)$$

The sun tab should never experience even half of this torque, so it will not fail. Similar calculations, shown by equation 10, reveal that the aluminum hard stop will also not fail.

$$\tau_{\max} = n_{\text{gear_ratio}} A_{\text{hardstop}} \sigma_{\text{UTS}} r_{\text{sun}} = (2.2)(1.35 \times 10^{-5} \text{ m}^2)(275 \text{ MPa})(0.01325 \text{ m}) = 108 \text{ Nm} \quad (10)$$

2.6 Preventing Failure Mechanically

Backlash in gears is essential for the elements to move smoothly, yet it often introduces added complexities and performance problems. For the case of the clutch, the backlash in the planetary actually helps the device to completely mesh the clutch plates during its operation. The clutch is designed to lock at zero angular velocity, exactly when the device reaches maximum extension. The backlash of the sun with respect to the ring is 1.6° and the backlash of the translating clutch plate's bosses within the mating planet carriers is 1° . This allows a maximum of 2.6° of movement within the clutch. This backlash plays an important role in limiting partial clutch plate engagements. If the clutch plates slam together at the tip fillets, the backlash will either allow the plates to rotate in the opposite direction of the angled teeth or slide down along the angled teeth to become fully meshed. In both cases, the control scheme of the solenoid is such that the solenoid continues to pull the clutch plates together until they are fully engaged. The machined aluminum tab on the solenoid mount, visible near the bottom of image b of figure 3, interfaces with an analog breakbeam sensor on the circuit board. The analog sensing regime of the breakbeam corresponds with the engagement of the clutch teeth, so the controls system is aware of the clutch plate configuration. The solenoid will therefore be commanded to continue to pull on the translating clutch plate until the plates are fully mated.

As previously mentioned, there is 1° of backlash between the translating clutch plate and its mating features in the planet carriers. This was implemented not only to increase the probability of complete clutch plate meshing, but also to reduce the possibility of binding. Binding could cause partial engagements or prevent clutch locking entirely. Mechanical wedging depends on geometry and friction. Figure 11 depicts the geometry that affects wedging in two dimensions. This same configuration can be used to assess the wedging of one of the solenoid mount legs that moves linearly through the planet carriers.

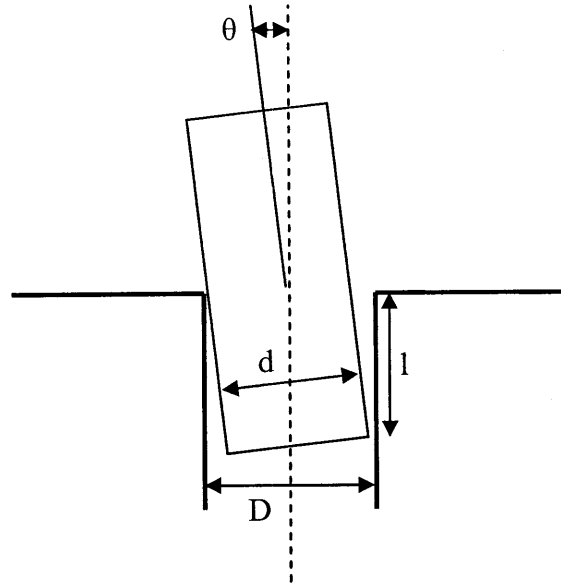


Figure 11: Geometry of wedging criterion.

Equation 11 uses the relations for wedging to identify the minimum angle at which wedging occurs, where μ is the coefficient of friction between the two surfaces [5]. The coefficient of friction of lubricated aluminum on aluminum contact is approximately 0.3.

$$\theta_{\text{wedging}} = \frac{D - d}{D\mu} = \frac{6.75\text{mm} - 6.31\text{mm}}{(6.75\text{mm})(0.3)} = 0.22\text{rad} = 12.4^\circ \quad (11)$$

The legs of the solenoid mount and the translating clutch plate will never bind in wedging because 12.4° is not physically reachable for the given configuration. Equation 12 shows that the maximum possible deviation is 1.3° because l is much greater than d .

$$\theta_{\text{max}} = \frac{(D - d)d}{Dl} = \frac{(6.75\text{mm} - 6.31\text{mm})(6.31\text{mm})}{(6.75\text{mm})(18\text{mm})} = 0.023\text{rad} = 1.3^\circ \quad (12)$$

Jamming is similar to wedging, but it accounts for insertion forces as well. This is a more realistic failure condition than wedging. The solenoid pulls with a maximum force of 35 N and its direction of pull is mainly directed by the iron plunger that is coaxial to it. The force actually drops out of the jamming equation, so the force angle, geometry, and friction are the only variables. Equation 13 calculates the force angle that is needed to cause jamming for the configuration shown in figure 12 [5].

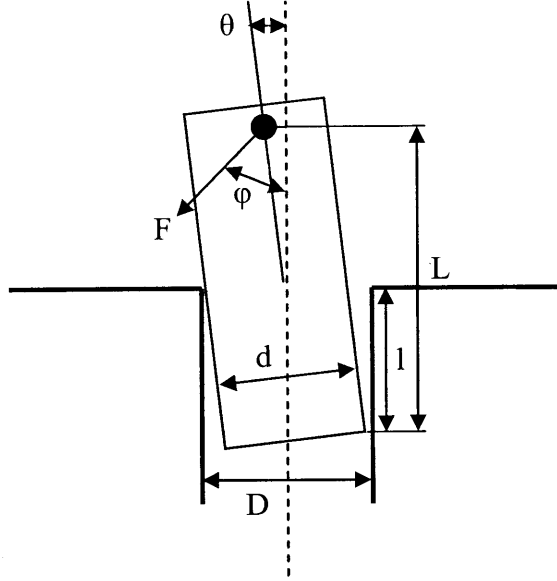


Figure 12: Geometry of jamming criterion.

$$\phi_{jam} = \tan^{-1} \left(\frac{1}{\mu \left(\frac{2L}{l} - \mu \frac{d}{l} - 1 \right)} \right) = \tan^{-1} \left(\frac{1}{(0.3) \left(\frac{(2)(24mm)}{18mm} - \frac{(0.3)(6.31mm)}{18mm} - 1 \right)} \right) = 1.13rad = 65^\circ \quad (13)$$

As in the previous case, the solenoid force can physically not be more than a few degrees off axis, so jamming is not possible. The rigid, cantilevered plunger concentric with the solenoid limits its movement, so this configuration can never be reached. A return spring is used to disengage the clutch plates by pushing on the solenoid, which is fixed to the solenoid mount and the translating clutch plate. There are no off axis forces in unlocking, so this should not be an issue. The legs of the solenoid mount and translating teeth should never bind in the planet carrier channels during the operation of the clutch.

3. Electronics

The electronics reside in the lateral part of the clutch, facing away from the user. The battery and circuit board are bolted into the lateral cap, which is held onto the clutch by two mating cylinders and two M3 screws. This subassembly is fully functional electronically, which is particularly useful for debugging purposes. Only one pair of wires links the lateral subassembly to the body of the clutch. There was no way to reconfigure the placement of the parts, so the solenoid wires are the only free wires in the system.

An AtMega168Pa AVR microcontroller operating at 12 MHz controls the clutch. A 2000 mAh lithium polymer battery is used to power the device for over 8 hours of continuous running. A dual axis MEMs accelerometer and a MEMs gyroscope provide acceleration and rotational rate sensing in the sagittal plane. The accelerometers are useful for detecting ground impact, while the gyroscope measures hip angular velocity.

All of the sensing is done optically and the features that enforce the lateral cap's placement ensure the proper positioning of the sensors. A reflective optical encoder reader is positioned to read the encoder that is fixed to a planet gear with a longer shaft. Reading the angular position of one of the planets means that higher resolution is gained over measuring the ring gear's position. An analog breakbeam sensor measures the position of the solenoid mount with respect to the clutch's main body to provide feedback on the configuration of the clutch plates for control purposes.

The lateral cap also features a power button and a mini USB port for data transfers and charging. Significant consideration was put into the placement of the electronics and sensors for ease of maintenance and reliability.

4. Controls

The mechanical system is also designed with the device's control's scheme in mind. All of the sensors for a robust control system are included, providing feedback on clutch plate position, knee angle, and the device's acceleration and rotational rates. Furthermore, the proper tolerancing of the clutch plates and gears dramatically improves the probability of full engagement. The basic control scheme of the clutch is diagrammed in figure 13. The controls scheme involves predicting the maximum angle of the clutch, as the latency of the solenoid is non-negligible, and locking at this angle. The system is held in the locked position by mechanical binding between the two clutch plates and it automatically releases at terminal stance when the joint is unloaded. At this time, the force of the return spring overcomes the frictional forces between the clutch teeth.

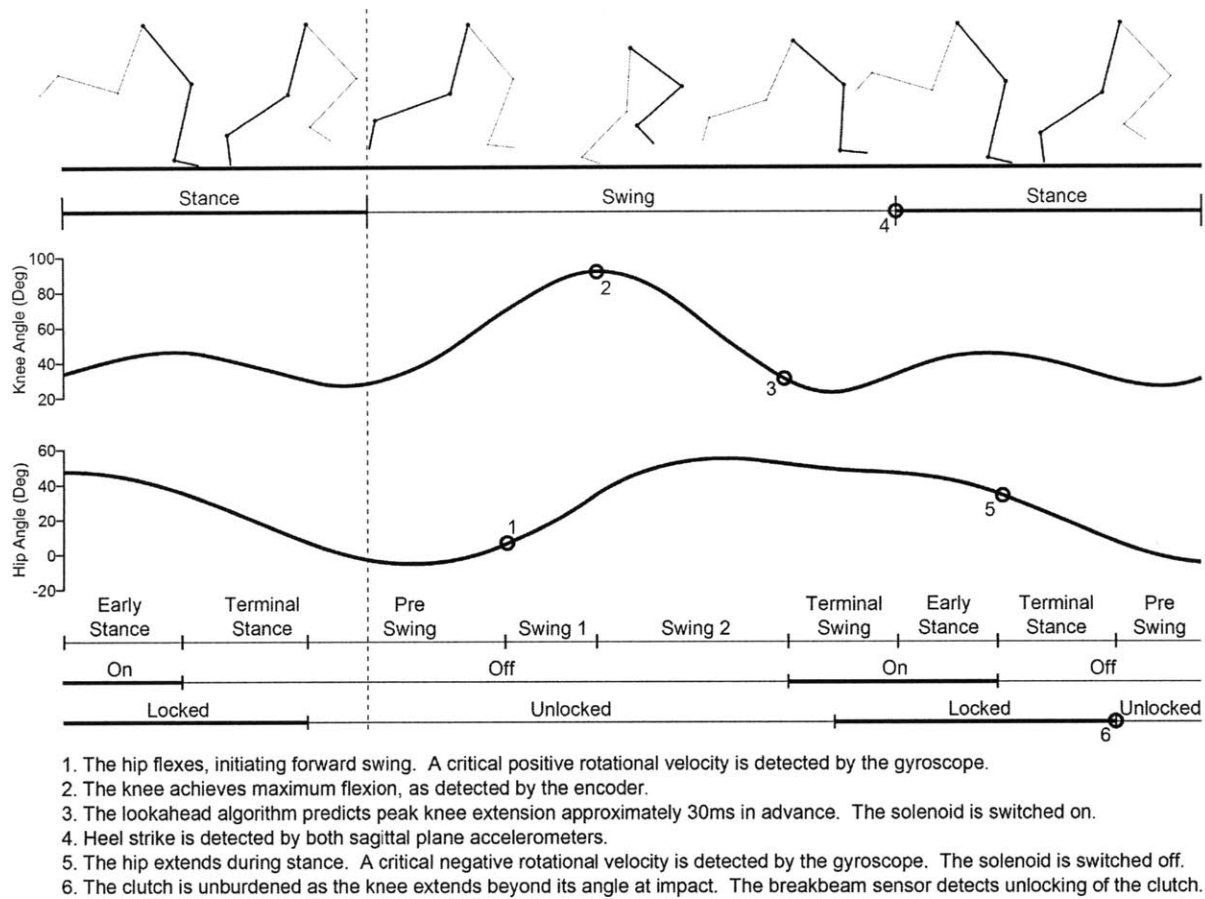


Figure 13: Diagram of biomechanics of running and the corresponding clutch control scheme.

5. Applications

This clutch will primarily be used in a compliant exoskeleton to augment human running. Figures 14 and 15 are images of initial testing of the running exoskeleton. This exoskeleton has the potential to be the first quasipassive device to augment human locomotion metabolically. Lightweight exoskeletons can also be of use to military personnel and emergency responders, who require mobility, speed, and load carrying augmentation.

This clutch can also be used in other prostheses, as these device could make use of lightweight, low power, high torque clutches. Even broader applications lie in integrating this clutch design into new braces and form fitting exoskeletons that can help to unload joints weakened by injuries or old age.



Figure 14: Two views of the exoskeleton during stance phase. Notice how the clutch is locked and energy is stored in the bowing leaf springs.

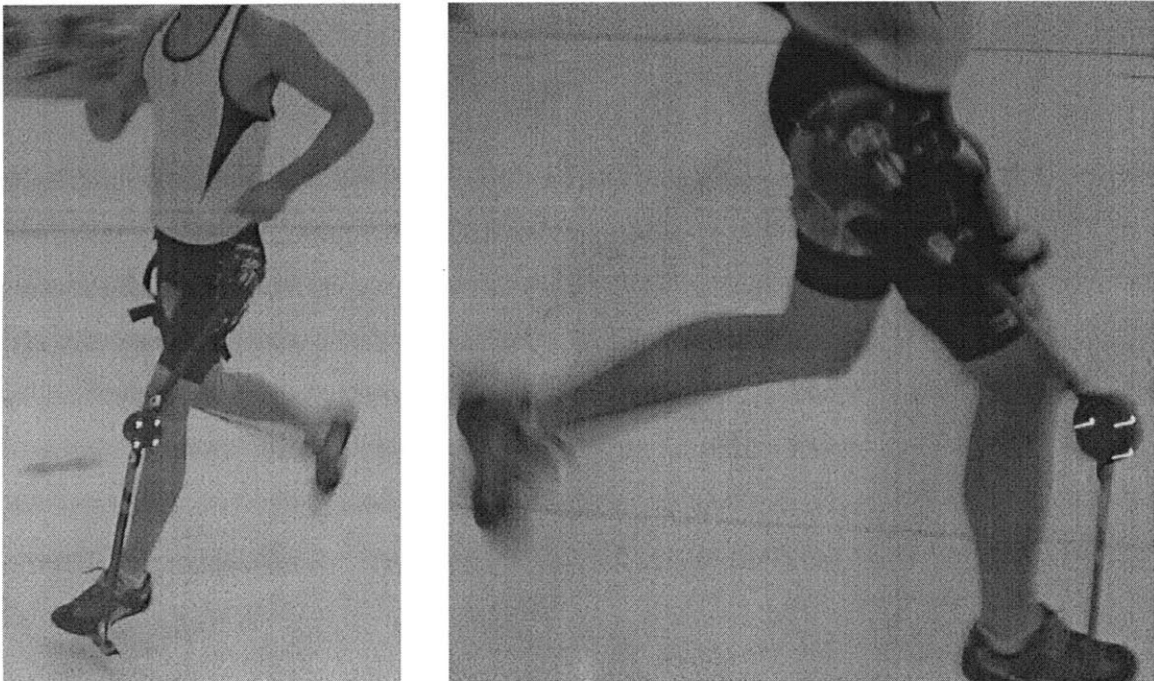


Figure 15: Two views of the harness that attaches the exoskeleton to the body.

References:

- [1] Grant A. Elliott. Compliant Exoskeleton for Augmentation of Human Running. Publication Pending, 2010.
- [2] Gear Stress. University of Washington. 2008. http://courses.washington.edu/mengr356/daly/Gear_stress.pdf.
- [3] R.C. Hibbler. *Mechanics of Materials*. New Jersey: Pearson Prentice Hall, 2005.
- [4] Material Property Data. *MatWeb* Automation Creations, Inc. Blacksburg, VA, 2010. <http://www.matweb.com>.
- [5] Daniel Whitney. Assembly Processes. 2008. https://stellar.mit.edu/S/course/2/fa08/2.008/courseMaterial/topics/topic3/lectureNotes/assembly_process08/assembly_process08.pdf.